

Table I. Chemical Shift and Charge Densities

DPN N =	chemical shift (δ)											
	C1	C2	C3	C4	C5	C6	C7	ipso	ortho	meta	para	
1	80.4							145.2	116.2	127.7	105.9	
	(-0.279)							(0.067)	(-0.091)	(-0.026)	(-0.143)	
3	90.2	127.9						145.4	117.5	128.1	111.3	
	(-0.227)	(-0.026)						(0.068)	(-0.081)	(-0.025)	(-0.114)	
5	96.5	134.6	98.2					143.9	119.4	128.0	115.0	
	(-0.193)	(0.010)	(-0.184)					(0.058)	(-0.071)	(-0.025)	(-0.095)	
7	102.4	133.7	101.5	140.5				142.7	120.8	128.1	117.7	
	(-0.163)	(0.005)	(-0.167)	(0.042)				(0.053)	(-0.064)	(-0.025)	(-0.080)	
9	107.4	133.2	105.4	139.8	103.3			141.7	121.9	128.2	119.7	
	(-0.135)	(0.003)	(-0.146)	(0.038)	(-0.157)			(0.048)	(-0.058)	(-0.024)	(-0.069)	
11	111.5	132.7	109.1	139.2	105.9	139.6		140.9	122.8	128.3	121.3	
	(-0.113)	(0.000)	(-0.126)	(0.035)	(-0.143)	(0.037)		(0.044)	(-0.053)	(-0.023)	(-0.061)	
13	114.9	132.3	112.5	138.6	108.6	139.0	107.5	140.3	123.4	128.3	122.5	
	(-0.095)	(-0.002)	(-0.108)	(0.032)	(-0.129)	(0.034)	(-0.135)	(0.041)	(-0.050)	(-0.023)	(-0.054)	

DP17. Surprisingly, the anions themselves exhibited no special tendency toward conformational diversity, despite the increasing availability of Z conformations with chain length. Indeed, ^1H NMR coupling constants were consistent with the all trans conformations for chains longer than C3. Homonuclear 2D (COSY) NMR spectroscopy allowed unambiguous assignment of proton chemical shifts in all cases, and heteronuclear ^{13}C - ^1H NMR spectroscopy thus allowed indirect assignment of ^{13}C chemical shifts. Linear least-squares treatment of the average charge density vs ^{13}C chemical shift (see Figure 1), excluding DP1, gave excellent statistics and allowed a calculation of individual charge densities at each site from the formula

$$\rho_{\text{C}} = (\delta_{\text{C}} - 132.7)/187.3 \quad (1)$$

The assigned chemical shifts and calculated charge densities are shown in Table I.^{8,9} More illustrative are these results plotted in histogram form. Figure 2 indicates the results for DP13. Included for the purpose of comparison are results from the calculated BCBS soliton model. As can clearly be seen, despite the delocalization that one might anticipate into the phenyl groups, negative charge accumulates in the center of the chain away from the ostensibly stabilizing phenyl groups. However, the diminution of charge with distance is less than that predicted by the 15 CH half-width of the SSH model but closer to that predicted by BCBS. Our solubility limitations prevent us from extrapolation to the limiting "true" soliton width. Although the amplitude of charge alternation in the phenyl-substituted anion is not as large as in the BCBS model, charge alternation remains a significant feature.

Although mechanisms for soliton generation and propagation are still under intense scrutiny, the predicted accumulation of charge within a fixed conjugation length thus appears to be validated by examination of resonance-stabilized carbanion models, even in a solvent, dimethyl sulfoxide, which minimizes counterion effects.¹⁰ The SSH Hamiltonian, a one-electron treatment, does not predict the charge alternation readily rationalized by mul-

ticonfigurational methods and now verified by ^{13}C nuclear magnetic resonance. However, its success at predicting the general structure as well as optical and magnetic properties of conducting polymers must be viewed as a vindication of one-dimensional calculational methods.

Acknowledgment. Support of this work by the Division of Materials Science, U.S. Department of Energy, through Grant No. DE-FG05-85ER45194 is gratefully acknowledged. We thank Les Gelbaum for the 400 MHz NMR measurements and Stuart Staley and Gideon Fraenkel for helpful discussions.

Synthesis and Characterization of a Soluble Oxide Inclusion Complex, $[\text{CH}_3\text{CN}(\text{V}_{12}\text{O}_{32}^{4-})]$

V. W. Day,*^{1a} W. G. Klemperer,*^{1b} and O. M. Yaghi^{1b}

Crystallitics Company
Lincoln, Nebraska 68501
Department of Chemistry
University of Illinois
Urbana, Illinois 61801
Received March 13, 1989

Microporous oxides such as zeolites have attracted widespread attention due to their ability to reversibly absorb small covalent molecules in a size- and shape-selective fashion.² The specificity associated with this inclusion phenomenon arises in part from the structural rigidity of the oxide host frameworks involved that impose correspondingly rigid geometric constraints on the guest molecules absorbed. To date, no molecular analogues of these solid oxide inclusion compounds have been reported, a surprising state of affairs given the existence of a wide variety of molecular inclusion complexes based on organic host molecules.³

The dodecavanadate inclusion complex $[\text{CH}_3\text{CN}(\text{V}_{12}\text{O}_{32}^{4-})]$ is prepared as a dark red, crystalline, tetra-*n*-butylammonium salt in >80% yield by refluxing an acetonitrile solution of $\text{V}_{10}\text{O}_{28}\text{H}_2[(n\text{-C}_4\text{H}_9)_4\text{N}]_4$ for 1-2 min, adding sufficient diethyl ether to obtain a precipitate, and recrystallizing the precipitate from 1:2 V/V acetonitrile/ethyl acetate at -5 °C. Although crystalline $[\text{CH}_3\text{CN}(\text{V}_{12}\text{O}_{32}^{4-})][(n\text{-C}_4\text{H}_9)_4]_4$, **1**, is unsuitable for X-ray structural analysis, suitable crystals of a solvated tet-

(1) (a) Crystallitics Company. (b) University of Illinois.

(2) (a) Barrer, R. M. In *Inclusion Compounds—Structural Aspects of Inclusion Compounds Formed by Inorganic and Organometallic Host Lattices*; Atwood, J. L., Davies, J. E. D., MacNicol, D. D., Eds.; Academic Press Inc.: London, 1984; Vol. 1, pp 191-248. (b) Maxwell, I. E. *J. Inclusion Phenom.* **1986**, *4*, 1.

(3) Lehn, J.-M. *Chem. Scr.* **1988**, *28*, 237.

(4) IR (Nujol, 500-1000 cm^{-1}) 524 (w), 551 (w), 611 (sh), 658 (vs), 714 (s), 758 (vs), 791 (sh), 861 (s), 994 (vs); ^{51}V NMR (0.02 M, 25 °C, CH_3CN) δ -590 (4V), -598 (4V), -606 (4V) relative to external VOCl_3 . Anal. Calcd for $\text{C}_{66}\text{H}_{147}\text{N}_5\text{V}_{12}\text{O}_{32}$: C, 37.14; H, 6.94; N, 3.28; V, 28.64. Found: C, 37.15; H, 6.94; N, 3.31; V, 28.59.

(8) For previous work on ^{13}C NMR studies of DP1, DP3, and related anions, see: (a) O'Brien, D. H. *Comprehensive Carbanion Chemistry, Part A*; Buncl, E., Durst, T., Eds.; Elsevier: 1980; p 271. (b) O'Brien, D. H.; Hart, A. J.; Russell, C. R. *J. Am. Chem. Soc.* **1975**, *97*, 4410. (c) O'Brien, D. H.; Russell, C. R.; Hart, A. J. *J. Am. Chem. Soc.* **1976**, *98*, 7427. (d) O'Brien, D. H.; Russell, C. R.; Hart, A. J. *J. Am. Chem. Soc.* **1979**, *101*, 633. (e) Bushby, R. J.; Ferber, G. J. *Tetrahedron Lett.* **1974**, 3701. (f) Bushby, R. J.; Ferber, G. J. *J. Chem. Soc., Perkin Trans. 2* **1976**, 1688. (g) Heiszwolf, G. J.; Kloosterziel, H. *Recl. Trav. Chim. (Pays-Bas)* **1967**, *86*, 1345. (h) Kloosterziel, H.; van Drunen, J. A. A. *Ibid.* **1968**, *87*, 1025.

(9) A referee has cautioned that the Spiess-Scneider correlation contains energy gap contributions to chemical shift anisotropies which may be difficult to separate from charge contributions. Such effects would show up in the slope of the plot of Figure 1. Thus the absolute magnitude of the charges may require some correction, but the relative charge densities will remain valid. For further discussion, see: (a) Tokuhira, T.; Fraenkel, G. J. *J. Am. Chem. Soc.* **1969**, *91*, 5005. (b) Grutzner, J. In *Recent Advances in Organic NMR Spectroscopy*; Lambert, J. B., Rittner, R., Eds.; Norell Press: Landisville, NJ, 1987; p 17-42.

(10) Matthews, W. S.; Bares, J. E.; Bartmess, J. E.; Bordwell, F. G.; Cornforth, F. J.; Drucker, G. E.; Margolin, Z.; McCallum, R. J.; McCollum, G. J.; Vanier, N. R. *J. Am. Chem. Soc.* **1975**, *97*, 7006.

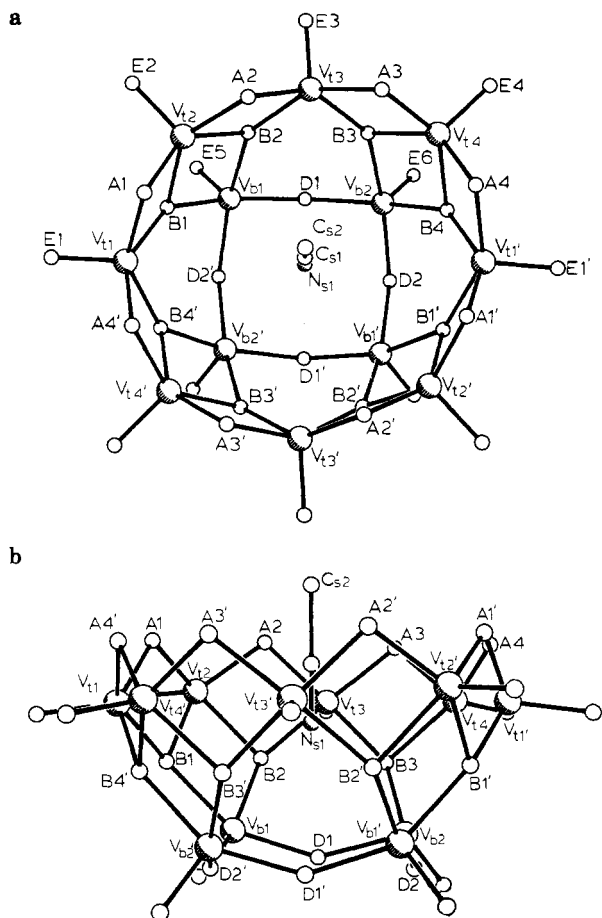


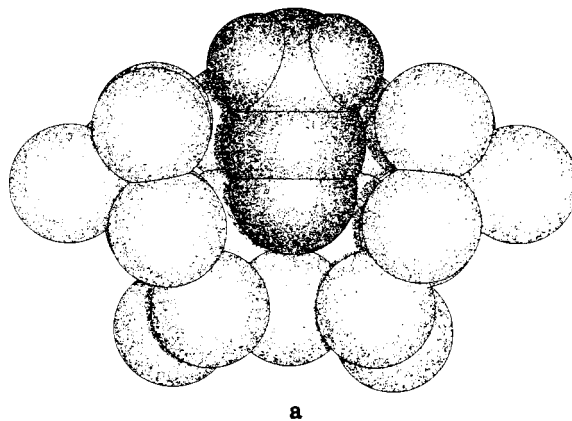
Figure 1. (a) Perspective plot of the non-hydrogen atoms for the $[\text{CH}_3\text{CNC}(\text{V}_{12}\text{O}_{32}^{4-})]$ anion as observed in crystalline $[(\text{C}_6\text{H}_5)_4\text{P}]_4\cdot 3\text{CH}_3\text{CN}\cdot 4\text{H}_2\text{O}$ (**2**). This view is nearly along the crystallographic 2-fold axis which passes through the bound acetonitrile molecule and relates primed and unprimed atoms. (b) Second perspective plot of the $[\text{CH}_3\text{CNC}(\text{V}_{12}\text{O}_{32}^{4-})]$ anion viewed approximately 90° away from the direction of Figure 1a and nearly perpendicular to the C_2 axis passing through the acetonitrile molecule. Vanadium and nitrogen atoms are represented by large- and medium-sized shaded spheres, respectively; oxygen and carbon atoms are represented by medium-sized open spheres. Oxygens which bridge two V_t vanadiums are labeled A, oxygens which bridge two V_t and one V_b vanadium are labeled B, and oxygens which bridge two V_b vanadiums are labeled D. Terminal oxygens are labeled E. Average values⁷ for structurally equivalent bond lengths of interest are as follows: $V_t\text{-O}_A$, 1.815 (6, 15, 26, 8) Å; $V\text{-O}_B$, 1.933 (5, 19, 41, 12) Å; $V_b\text{-O}_D$, 1.804 (6, 17, 20, 4) Å; $V\text{-O}_E$, 1.586 (7, 7, 13, 6) Å; $N_{s1}\text{-C}_{s1}$, 1.111 (14) Å and $C_{s1}\text{-C}_{s2}$, 1.490 (16) Å.

raphenylphosphonium salt could be obtained from **1** plus excess $[(\text{C}_6\text{H}_5)_4\text{P}]\text{Br}$ in acetonitrile.

X-ray structural analysis⁵ of crystalline $(\text{V}_{12}\text{O}_{32})[(\text{C}_6\text{H}_5)_4\text{P}]_4\cdot 4\text{CH}_3\text{CN}\cdot 4\text{H}_2\text{O}$, **2**, revealed the presence of $(\text{C}_6\text{H}_5)_4\text{P}^+$ cations, water, and acetonitrile molecules of crystallization and discrete $[\text{CH}_3\text{CNC}(\text{V}_{12}\text{O}_{32}^{4-})]$ complexes having the structure shown in

(5) Single crystals of $[(\text{CH}_3\text{CN})\text{V}_{12}\text{O}_{32}][(\text{C}_6\text{H}_5)_4\text{P}]_4\cdot 3\text{CH}_3\text{CN}\cdot 4\text{H}_2\text{O}$ (**2**) are at $20 \pm 1^\circ\text{C}$ monoclinic, space group $C2/c\text{-}C_{2h}^2$ (no. 15) with $a = 41.814$ (7) Å, $b = 13.556$ (3) Å, $c = 27.198$ (5) Å, $\beta = 128.60$ (1°), and $Z = 4$ formula units [$d_{\text{calc}} = 1.498$ g cm^{-3} ; μ_a (Mo $K\alpha$) = 0.98 mm^{-1}]. A total of 8274 unique reflections having 2θ (Mo $K\alpha$) $< 45.80^\circ$ were collected on a Nicolet P1 auto diffractometer by using graphite-monochromated Mo $K\alpha$ radiation and full 0.90° -wide ω scans. The structure was solved by using (SHELXTL) "direct methods" techniques, and the resulting structural parameters⁶ have been refined by using counter-weighted cascade block-diagonal least-squares techniques to R_1 (unweighted based on F) = 0.048 and R_2 (weighted, based on F) = 0.060 for 4466 independent reflections having 2θ (Mo $K\alpha$) $< 45.8^\circ$ and $I > 3\sigma(I)$. These refinement cycles employed anisotropic thermal parameters for all non-hydrogen atoms and fixed isotropic thermal parameters for phenyl hydrogens at idealized positions in the $(\text{C}_6\text{H}_5)_4\text{P}^+$ cations. It was not possible to locate hydrogen atoms on the acetonitrile or water molecules.

Figure 1, where an acetonitrile molecule is suspended in the center of a basket-like $\text{V}_{12}\text{O}_{32}^{4-}$ cage. Although the $\text{V}_{12}\text{O}_{32}^{4-}$ cage rigorously possesses only crystallographic C_2 symmetry, it approximates C_{4h} symmetry but is elliptically distorted such that the $\text{O}_{A1}\cdots\text{O}_{A1'}$ and $\text{O}_{A2}\cdots\text{O}_{A2'}$ distances of 6.848 (8, 46, 46, 2) Å are significantly shorter than the $\text{O}_{A3}\cdots\text{O}_{A3'}$ and $\text{O}_{A4}\cdots\text{O}_{A4'}$ distances of 7.445 (8, 3, 3, 2) Å. The four V_b vanadiums in the "bottom of the basket" are coplanar to within 0.04 Å, and the eight V_t vanadiums at the "top of the basket" are coplanar within 0.17 Å. The vanadium coordination geometry within the $\text{V}_{12}\text{O}_{32}^{4-}$ cage framework is similar to that observed in square-pyramidal vanadium(V) compounds such as orthorhombic V_2O_5 ⁸ and $\alpha\text{-VOPO}_4$.⁹ The acetonitrile molecule forms only extremely weak bonds to vanadium [$d_{N_{s1}\text{-}V_b} = 3.283$ (9, 20, 20, 2) Å, $d_{N_{s1}\text{-}V_t} = 3.747$ (9, 74, 149, 4)] and has long nonbonding contacts with the $\text{V}_{12}\text{O}_{32}^{4-}$ cage [$d_{C_{s1}\text{-}O_A} = 3.604$ (8, 140, 160, 4) Å, $d_{N_{s1}\text{-}O_B} = 3.367$ (8, 51, 83, 4) Å, $d_{N_{s1}\text{-}O_D} = 3.341$ (8, 56, 56, 2) Å] as shown in the space-filling model **a**.¹⁰ Nonetheless, the acetonitrile molecule



remains largely associated with the $\text{V}_{12}\text{O}_{32}^{4-}$ anion in solution: a 13 mM solution of **1** in $\text{C}_6\text{D}_5\text{NO}_2$ shows ^1H NMR resonances for free acetonitrile (δ 2.08) and bound acetonitrile (δ 2.38) with relative intensities of about 1:2, respectively, at 8°C . It is perhaps significant that the average $N_{s1}\text{-}V_b\text{-}O_E$ angle of 177.4 (4, 3, 3, 2) $^\circ$ approaches 180° : the $\text{V}_{12}\text{O}_{32}^{4-}\text{-CH}_3\text{CN}$ host-guest interaction thus may be analogous to the interaction between square-pyramidal V(V) in layered vanadates such as $\alpha\text{-VOPO}_4$ and intercalated ligands such as pyridine.¹¹

The *nido*- $\text{V}_{12}\text{O}_{32}^{4-}$ cage framework is a new structure type that can be derived from two different types of closo cage frameworks previously observed in polyoxovanadate structures. The vanadium(V) heteropolyanion $\text{PV}_{14}\text{O}_{42}^{9-12}$ contains a PO_4^{3-} anion surrounded by a *closo*- $\text{V}_{14}\text{O}_{38}^{6-}$ cage based on the rhombicuboctahedron,^{13,14} an Archimedean polyhedron. The vanadium(IV) compound $\text{K}_{12}\text{V}_{18}\text{O}_{42}\cdot 16\text{H}_2\text{O}$ ¹⁵ contains a water molecule surrounded by a *closo*- $\text{V}_{18}\text{O}_{42}^{12-}$ cage based on the so-called "fourteenth Archimedean polyhedron", the elongated square gyrobicupola.¹⁶ The $\text{V}_{12}\text{O}_{32}^{4-}$ framework is in fact closely related

(6) See paragraph at end of paper regarding Supplementary Material.

(7) The first number in parentheses following an average value of a bond length or angle is the root-mean-square estimated standard deviation of an individual datum. The second and third numbers are the average and maximum deviations from the average value, respectively. The fourth number represents the number of individual measurements which are included in the average value.

(8) Enjalbert, R.; Galy, J. *Acta Crystallogr. Sect. C* **1986**, *C42*, 1467.

(9) Jordan, B.; Calvo, C. *Can. J. Chem.* **1973**, *51*, 2621.

(10) In **a**, methyl hydrogen atoms were generated assuming an arbitrary orientation of the CH_3CN molecule about the crystallographic C_2 axis, with 1.1 Å C-H bond lengths and 109.5° H-C-H bond angles. Van der Waals radii were used for carbon (1.70 Å), hydrogen (1.20 Å), nitrogen (1.50 Å), and oxygen (1.40 Å) atoms.

(11) Johnson, J. W.; Jacobson, A. J.; Brody, J. F.; Rich, S. M. *Inorg. Chem.* **1982**, *21*, 3820.

(12) Kato, R.; Kobayashi, A.; Sasaki, Y. *Inorg. Chem.* **1982**, *21*, 240.

(13) Wells, A. F. *Structural Inorganic Chemistry*, 5th ed.; Clarendon Press: Oxford, 1984; pp 71-74.

(14) Polyoxocuprates based on the rhombicuboctahedron are also known: Kepka, R.; Müller-Buschbaum, H. *Z. Naturforsch.* **1977**, *32B*, 121, 124.

(15) Johnson, G. K.; Schlemper, E. O. *J. Am. Chem. Soc.* **1978**, *100*, 3645.

to V_2O_5 sheets in the orthorhombic V_2O_5 layer structure,⁸ raising the possibility that other *nido*-polyoxoanion cages might be derived from other layered structures such as the α -VOPO₄ structure.

Preliminary investigations indicate that the $V_{12}O_{32}^{4-}$ host is quite robust and is likely to form a variety of different inclusion complexes not only with other uncharged guest molecules but also with anions capable of bonding to vanadium(V) centers and cations capable of interacting with anionic oxygen centers. Moreover, molecular analogues of redox intercalation reactions of layered compounds such as VOPO₄·2H₂O¹⁷ or V_2O_5 ¹⁸ may be possible since the cyclic voltammogram of compound **1** in CH₃CN shows a reversible wave with $E_{1/2} = -0.52$ V vs F_c^+/F_c^- .

Acknowledgment. We acknowledge the National Science Foundation for support of this work. Chris Frank provided invaluable technical assistance.

Supplementary Material Available: Crystal structure analysis report, Table I (atomic coordinates for non-hydrogen atoms), Table II (anisotropic thermal parameters for non-hydrogen atoms), Table III (atomic coordinates for hydrogen atoms of the cations), Table IV (bond lengths and bond angles for the anion), Table V (bond lengths and bond angles for the cations), Table VI (bond lengths and bond angles for acetonitrile solvent molecules), Figure 2 (parts a and b) (perspective ORTEP plots of $(C_6H_5)_4P^+$ cations), Figure 3 (perspective ORTEP plots of the non-hydrogen atoms of acetonitrile molecules), and Figure 4 (perspective ORTEP plot of the anion) (28 pages); table of observed and calculated structure factors for $[(CH_3CN)V_{12}O_{32}][C_6H_5)_4P]_4 \cdot 3CH_3CN \cdot 4H_2O$ (20 pages). Ordering information is given on any current masthead page.

(16) Johnson, N. W. *Can. J. Math.* **1966**, *18*, 169.

(17) Jacobson, A. J.; Johnson, J. W.; Brody, J. F.; Scanlon, J. C.; Lewandowski, J. T. *Inorg. Chem.* **1985**, *24*, 1782.

(18) Murphy, D. W. In *Intercalation Chemistry*; Whittingham, M. S., Jacobson, A. J., Eds.; Academic Press: New York, 1982; pp 563-572.

Stereospecific Hydrolysis of Alkyl Esters by Antibodies

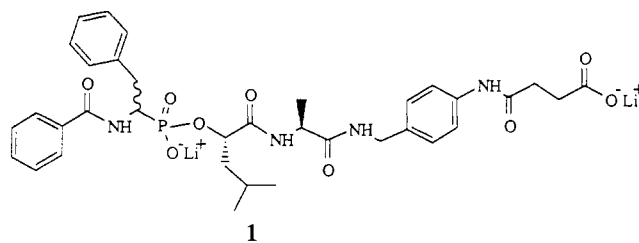
Scott J. Pollack, Paul Hsiun, and Peter G. Schultz*

Department of Chemistry, University of California
Berkeley, California 94720

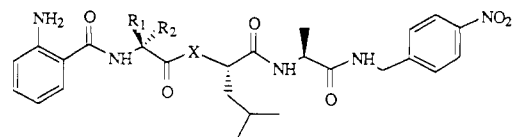
Received April 4, 1989

Enzymes are playing an increasingly important role as catalysts in chemistry, due to their ability to catalyze highly selective transformations of complex polyfunctional molecules.¹ However, in many cases enzymes are unavailable for a specific reaction of interest. We² and others³ have recently demonstrated that the high binding specificity of the immune system can be exploited to develop new biological catalysts with tailored specificities. Antibodies have been generated with catalytic groups in the binding site,⁴ with cofactor binding sites,⁵ semisynthetic antibodies have been generated,⁶ and the notions of approximation⁷ and

transition state stabilization^{2,3,8} have been applied to the generation of catalytic antibodies. We now report application of the latter strategy to the generation of antibodies which catalyze the *stereospecific* hydrolysis of *alkyl* esters.⁹ Antibodies generated to phosphonate hapten **1** were found to catalyze the hydrolysis of ester **2** with a greater than 200/1 preference for the (*R*)-phenylalanine-containing isomer relative to the (*S*)-phenylalanine-containing isomer.



Antibodies were generated against hapten **1**, a tripeptide transition state analogue for the hydrolysis of ester **2** or peptide **3** under basic conditions. Hapten **1** was synthesized as a roughly equimolar mixture of two diastereomers and coupled via its carboxylic acid to the carrier protein keyhole limpet hemocyanin¹⁰ in order to elicit an immune response.¹¹ Note that the hapten also contains analogues of fluorogenic groups which allow hydrolysis of substrates **2** and **3** to be monitored by observing the fluorescence increase which occurs when the fluorescent 2-aminobenzoyl group is separated from the quenching 4-nitrobenzylamide in the reaction.¹² (This sensitive assay may allow direct screening of ELISA plates for catalytic activity.)



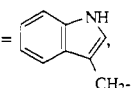
2a: $R_1 = H, R_2 = PhCH_2-, X = O$

2b: $R_1 = PhCH_2-, R_2 = H, X = O$

3a: $R_1 = H, R_2 = PhCH_2-, X = NH$

3b: $R_1 = PhCH_2-, R_2 = H, X = NH$

4: $R_1 = H, R_2 = (CH_3)_2CHCH_2-, X = O$

5: $R_1 = H, R_2 =$  $, X = O$

Ester hydrolysis was monitored by fluorescence measurement with a Perkin-Elmer LS 5B spectrophotometer using 340 nm for excitation and 415 nm for emission. Reactions were carried out in 0.2 M borate, 0.15 M sodium chloride (BBS), pH 8.0, at 24 °C, in the presence of 3.33 μ M antibody.¹³ Although none of the 31 IgGs¹⁴ specific for **1** accelerated the hydrolysis of peptide

(8) (a) Jackson, D. Y. et al. *J. Am. Chem. Soc.* **1988**, *110*, 4841. (b) Hilvert, D. et al. *Proc. Natl. Acad. Sci. U.S.A.* **1988**, *85*, 4953.

(9) The recent observation of catalytic antibodies which stereospecifically hydrolyze unactivated esters of chiral alcohols was independently reported by Benkovic and co-workers.²⁰

(10) Jacobs, J.; Schultz, P. G.; Sugawara, R.; Powell, M. *J. Am. Chem. Soc.* **1987**, *109*, 2174.

(11) Swiss Webster mice were immunized with the KLH-1 conjugates. A fusion was carried out by standard methods by using SP2/0 myeloma as a fusion partner.²¹

(12) Nishino, N.; Powers, J. C. *J. Biol. Chem.* **1980**, *255*, 3482.

(13) Reactions were initiated by adding a stock solution (dimethyl sulfoxide) of the ester substrate **2** (5 μ L) to the antibody in 0.5 mL of reaction buffer. Fluorescence values for hydrolysis products were calibrated by alkaline hydrolysis (pH 12, by addition of 7 N NaOH [10 μ L] to the reaction mixture) followed by adjustment of the pH to assay conditions with 12 N HCl and correcting for dilution. The fluorescence changes upon complete hydrolysis showed a consistent linear dependence on substrate concentration up to 50 μ M substrate. Protein molarity was determined from A_{280} ($E_{1cm}^{0.1\%} = 1.37$) and a molecular weight of 150 000 for IgG.

* Author to whom correspondence should be addressed.

(1) Whitesides, G. M.; Wong, C. *Angew. Chem., Int. Ed. Engl.* **1985**, *24*, 617.

(2) (a) Pollack, S. J.; Jacobs, J. W.; Schultz, P. G. *Science* **1986**, *234*, 1570.

(b) Jacobs, J. W.; Schultz, P. G.; Sugawara, R.; Powell, M. *J. Am. Chem. Soc.* **1987**, *109*, 2174.

(3) Tramontano, A.; Janda, K. D.; Lerner, R. A. *Science* **1986**, *234*, 1566.

(4) (a) Cochran, A. G.; Sugawara, R.; Schultz, P. G. *J. Am. Chem. Soc.* **1988**, *110*, 7888. (b) Shokat, K. M.; Leumann, C. J.; Sugawara, R.; Schultz, P. G. *Nature (London)* **1989**, *338*, 269.

(5) (a) Shokat, K. M.; Leumann, C. H.; Sugawara, R.; Schultz, P. G. *Angew. Chem., Int. Ed. Engl.* (b) Iverson, B. L.; Lerner, R. A. *Science* **1989**, *243*, 1184.

(6) (a) Pollack, S. J.; Nakayama, G. R.; Schultz, P. G. *Science* **1988**, *242*, 1038. (b) Pollack, S. J.; Schultz, P. G. *J. Am. Chem. Soc.* **1989**, *111*, 1929.

(7) Napper, A. D.; Benkovic, S. J.; Tramontano, A.; Lerner, R. A. *Science* **1987**, *237*, 1041.